Nonlinear microwave response of YBaCuO superconducting film

E. S. Borovitskaya, and V. M. Genkin

Institute of Physics of Microstructures, Russian Academy of Sciences, Nizhnii Novgorod, Russia

G. I. Leviev

Institute of Solid State Physics, Russian Academy of Sciences, 142432 Chernogolovka, Moscow Region, Russia

(Submitted 2 February 1996)
Zh. Éksp. Teor. Fiz. **110**, 1081–1094 (September 1996)

Generation of the third harmonic by a normal microwave magnetic field in a thin YBaCuO film has been studied theoretically and experimentally. Unlike measurements in the rf band, the harmonic generation has no threshold. The harmonic intensity as a function of temperature at low incident wave amplitude is controlled by the temperature dependence of the penetration depth, $\lambda(T)$, and the former parameter can be employed in experimental studies of the latter. The experimental data have been interpreted in terms of a relationship between the superconducting current and the condensate velocity different from that suggested by the Ginzburg–Landau theory. © *1996 American Institute of Physics.* [S1063-7761(96)02309-8]

1. INTRODUCTION

The microwave response of a superconductor is nonlinear. As a result, several effects can be detected in superconductors, such as a frequency dependence of the sample impedance,[1–5] variations in the critical current due to microwave field, and higher harmonics in the spectrum of a reflected wave. We have focused our attention on the latter.

Harmonic generation has been analyzed in traditional superconductors from different viewpoints.[6–10] The relaxation time of the order parameter was derived from the temperature dependence of the third-harmonic power generated in YBaCuO single crystals.[11] The nonlinearity leading to generation of a second harmonic in ceramic samples was studied by Ciccarello *et al.*[12] using Bean's model. Generation of the second harmonic in a mixed state was theoretically investigated by Coffey and Clem.[13] Ji *et al.*.[14] studied a third harmonic generated in ceramic samples in the band extending from 500 Hz to 50 kHz both theoretically and experimentally. In their recent publication, Ciccarello *et al.*[15] reported on generation of a third harmonic in a YBaCuO single crystal at high pump power, when the response is highly nonlinear and the third-harmonic amplitude is not proportional to the cube of the incident power. The experimental results were interpreted in terms of the superconducting electron concentration proportional to the absolute value of the pump amplitude, and that of a higher harmonic is determined by the appropriate Fourier component of the microwave field averaged over the sample volume.

In this paper we report on the generation of the third harmonic in a thin YBaCuO epitaxial film. The detector sensitivity was high enough to perform measurements at low amplitudes of the incident field, when the third-harmonic amplitude is proportional to the cube of the incident-wave amplitude, although the available dynamic range of such measurements is rather low. At higher amplitudes and temperatures far from the critical value, the third-harmonic amplitude grew with the incident field intensity faster than its third power, and at temperatures close to the superconducting transition slower than the third power.

The mechanism of harmonic generation in the range of cubic dependence is likely to be related to the nonlinearity in the Ginzburg–Landau equations. In the phenomenological theory, the superconducting component of a uniform, steady-state current in a thin film has the form

$$j_s = -\frac{c}{4\pi\lambda^2}\left(A - \frac{\Phi_0}{2\pi}\nabla\phi\right)(1-G), \tag{1}$$

where

$$G = \frac{4}{27}\frac{(A-\Phi_0/2\pi\nabla\phi)^2 c^2}{(4\pi\lambda^2 j_{GL})^2}.$$

Here Φ_0 is the magnetic flux quantum, A is the external field vector potential, ϕ is the phase of the superconducting order parameter, and j_{GL} is the Ginzburg–Landau decoupling current.

In order to calculate the radiation power, we have used the standard theory of microwave cavities driven by an external current,[16] which is, in our opinion, preferable to that using the field averaged over the cavity because it allows us to describe correctly the radiation intensity as a function of the sample size.

2. EXPERIMENTAL TECHNIQUES

A 100-nm YBaCuO film was manufactured by laser ablation on a substrate of neodymium gallate. The sample c axis was aligned with the substrate normal. Then the sample was cut into two approximately equal parts and a lithographic pattern was fabricated on each of them. A pattern of superconducting circles with a diameter of 1 mm and a distance of 2 mm between their centers was produced on one part, and a similar pattern with dimensions a factor of ten smaller was made on the other part of the substrate. Measurements were performed either with one 1-mm circle or with ten 0.1-mm circles.

 1063-7761/96/090597-08$10.00

The tested sample was placed in a bimodal cylindrical cavity resonant at 9.2 GHz in the E_{010} mode and at triple that frequency in the H_{011} mode. The cavity bottom was a contactless plunger, which allowed us to tune the H_{011} mode to triple the frequency of the E_{010} mode (the frequency of the E_{010} mode was essentially constant with plunger position). The cavity was coupled to the waveguides via two perpendicular slits cut through in the cavity lid. Parasitic higher harmonics generated by the magnetron could be easily filtered out by harmonic filters.

It was more difficult to suppress harmonic generation at contacts between components of the microwave circuit. It was desirable either to braze these connections in order to have good conducting contacts or to insulate them from one another with a thin Teflon film. The freshly fabricated cavity was trained for some time under a high microwave field without a sample. Small metallic particles remaining in the cavity after washing burned in the process, and parasitic signals due to these particles were eliminated.

The cavity was driven by the electromagnetic field of a pulsed magnetron which produced microwave pulses with a width of 2 μs. The duty factor was set high enough for the signal to be independent of the separation between pulses. The maximum pulsed power fed to the cavity was at most several kilowatts. The power was smoothly varied by an attenuator driven by an electric motor and measured by a thermistor bridge to within several percent. The harmonic generated in the sample was coupled into a waveguide of smaller cross section that was cutoff for the first harmonic, and fed to the input of a superheterodyne detector. Its output was processed by a boxcar integrator and fed to a computer. The temperature controller allowed us either to scan the temperature at a desired rate or to maintain it at a constant value. The experimental facility could either generate a dc magnetic field of up to 200 Oe or compensate for the earth's magnetic field.

The sample position within the cavity and its alignment were selected so that the magnetic fields of both resonant modes were aligned with the sample normal. Note that in this configuration the intensity of the third harmonic generated in the sample is higher than in the case of a microwave field parallel to the sample plane. The signal could be also recorded as a function of dc magnetic field.

3. EXPERIMENTAL RESULTS

We have measured the third-harmonic amplitude at various temperatures and ac magnetic field amplitudes. Measurements could be performed at temperatures ranging between liquid helium and room temperature; our attention, however, was focused on the range around the superconducting transition. Figure 1 shows the third-harmonic amplitude versus temperature at fixed incident-wave amplitude. The coincidence of the two peaks indicates that they are determined not by geometrical parameters, but by inherent properties of the films. The experimental curves of the third-harmonic amplitude $H_{3\omega}$ as a function of the incident field amplitude for the smaller film are given in Figs. 2–4.

One can see that at lower amplitudes the experimental points lie on a third-power curve, whereas at higher amplitudes the experimental curve deviates from the cubic curve toward higher intensities at lower temperatures (Fig. 2) and vice versa (Fig. 4). Similar effects were detected in the circles of larger diameter (Figs. 3 and 5). An important point is that all the curves described here were recorded at temperatures below the peak in Fig. 1.

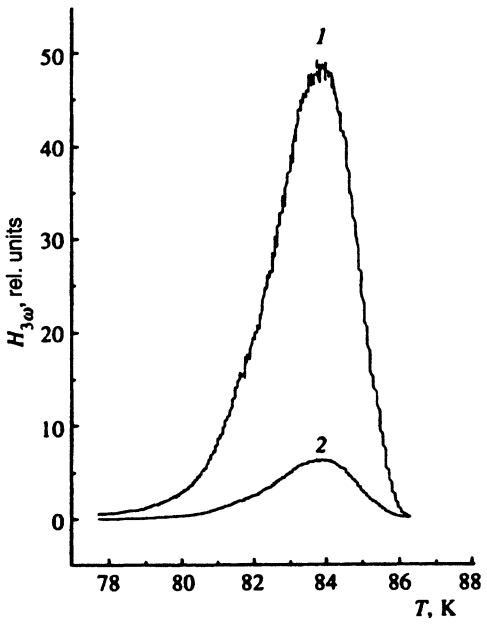

FIG. 1. Amplitude of the third harmonic plotted against temperature: curve *1* refers to the larger film, curve *2* to the smaller film.

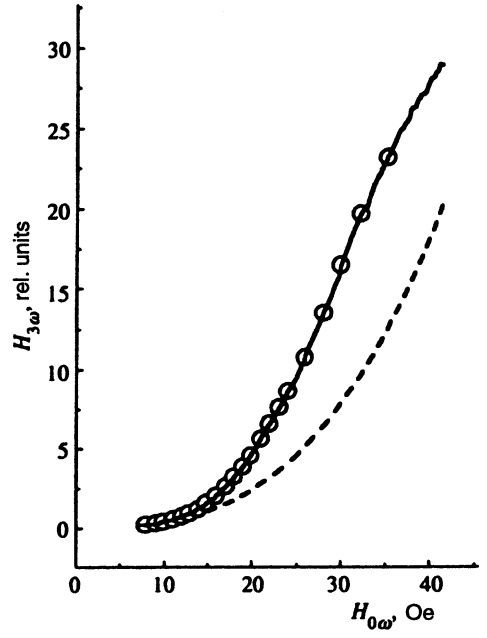

FIG. 2. Amplitude of the third harmonic versus incident microwave-field amplitude in the smaller film at low temperatures. The circles show experimental points measured at $T=78.8$ K, the solid line is a theoretical curve at $T=78.8$ K, the dashed line shows the cubic function.

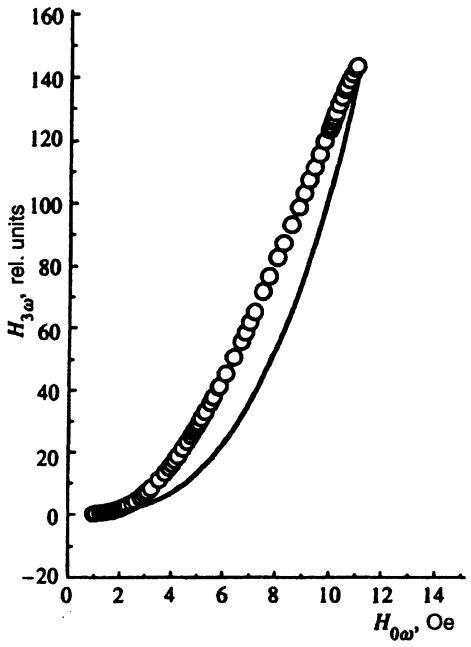

FIG. 3. Amplitude of the third harmonic versus incident microwave-field amplitude in the larger film at low temperatures. The circles are experimental points at $T=79.5$ K, the solid line shows the cubic function.

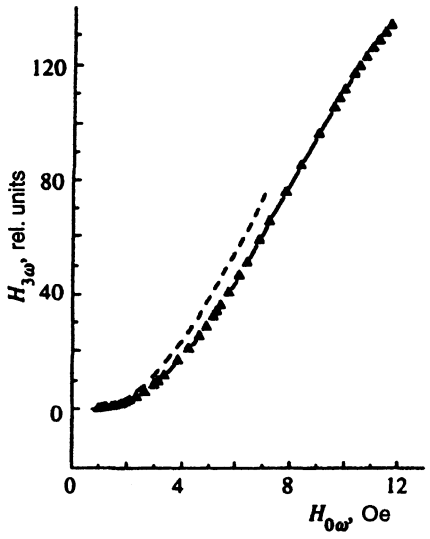

FIG. 5. Amplitude of the third harmonic generated in the larger film as a function of microwave field amplitude at high temperatures, $T=82.1$ K (triangles, the solid line connects experimental points); the dashed line shows the cubic function.

4. THEORETICAL MODEL

4.1. Linear response

A circular thin film in a magnetic field perpendicular to its surface was studied by analytic methods by Mikheenko and Kuzovlev,[17] but for our purpose it is more convenient to use an alternative method,[18] although it demands numerical calculations. It will be demonstrated below that the technique enables one to get rid of divergences in the current and vector potential at the film edge.

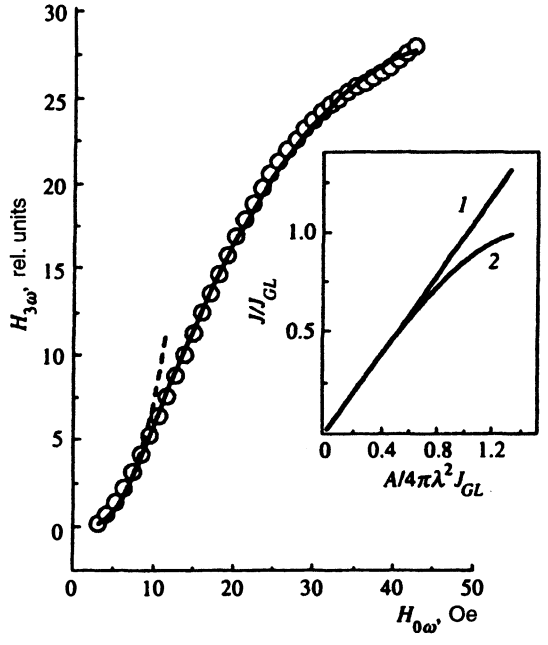

FIG. 4. Amplitude of the third harmonic generated in the smaller film versus incident microwave-field amplitude at high temperatures, $T=82.5$ K; the points are experimental points, the solid line shows calculations, and the dashed line the cubic function. The insert is the current plotted against the vector potential: curve *1* shows the function which yields the best fit to the experimental points at $T=82.5$ K, and curve *2* shows the function derived from the Ginzburg–Landau theory.

Consider a circular film of radius R much smaller than the incident wavelength in a microwave cavity. In order to compare our calculations with experimental results, we discuss the specific case of a bimodal cylindrical cavity resonant at the fundamental frequency in the E_{010} mode and at triple that frequency in the H_{111} mode. The sample is oriented perpendicular to the microwave fields of both modes. Given a cavity with a quality factor Q_ω, an incident microwave field of frequency ω and power p_ω generates on the sample surface an electromagnetic field with vector-potential amplitude $A_{\omega 0}=k\sqrt{p_\omega Q_0}$, where k is a geometric factor. This field generates eddy currents in the film such that the total vector potential $A_\omega(r)$ is cylindrically symmetrical and described by the equation[19]

$$-\nabla^2\mathbf{A}_\omega+\frac{1}{\Lambda}\delta(z)\left(\mathbf{A}_\omega-\frac{\Phi_0}{2\pi}\nabla\phi\right)=\frac{4\pi}{c}\mathbf{j}^{\text{ext}}+\mathbf{g}(r). \quad (2)$$

Here we assume that the film is in the plane $z=0$. Since the external field has only a z-component, the vector potential A_ω and current j have only θ-components, owing to the cylindrical symmetry. In Eq. (2) $\Lambda=\lambda^2/d$, where λ is the magnetic field penetration range and d is the film thickness. We assume that the film is located in the uniform magnetic field $H_{0\omega}$ generated by the current j^{ext} in a solenoid of radius $R_0\gg R$. We demonstrate below that the result is independent of R_0. The function $\mathbf{g}(r)$ on the right-hand side of Eq. (2) has the form

$$\mathbf{g}(r)=\left[\frac{\Phi_0}{2\pi}\nabla\phi+\frac{c^2}{108\pi^2\lambda^4 j_{GL}^2}\left(\mathbf{A}_\omega-\frac{\Phi}{2\pi}\right)^3\right]\frac{\theta(R-r)}{\Lambda}, \tag{3}$$

where $\Lambda=\lambda^2/d$ is Pearl's magnetic field penetration range in a superconducting film.[19]

It is noteworthy that in this form the equation also enables one to calculate the current distribution in the presence of vortices that penetrate a sample at a current higher than the decoupling current. If a film contains vortices, then $\nabla\phi \neq 0$, and Eq. (2) should be supplemented with equations of the vortex dynamics. In a superconducting strip of thickness $d\gg\lambda$, the problem was solved by Zeldov *et al.*[21] and by Indenbom and Brandt.[22] The problem of vortices in a film of thickness $d\ll\lambda$ in a perpendicular magnetic field was studied by Likharev,[23] who demonstrated that penetration starts at a field in which the Meissner current density at the edge is equal to the decoupling current. The dynamics of vortices in a circular thin film was discussed previously.[18] We demonstrate below, however, that vortices are not generated at microwave powers used in this work, so we can take $\nabla\phi=0$ in Eq. (2).

We solve Eq. (2) using a numerical technique described elsewhere.[24] Let us take Fourier components

$$\mathbf{A}_\omega(r,z)=\sum_{k,q}\mathbf{A}_{kq}\exp(i\mathbf{q}\cdot\mathbf{r}+ikz), \tag{4}$$

and thus transform Eq. (2) to the following form:

$$\mathbf{A}_{kq}+\frac{2\pi R}{\Lambda(k^2+q^2)}\sum\frac{J_1(|\mathbf{q}-\mathbf{q}'|R)}{|\mathbf{q}-\mathbf{q}'|}\mathbf{A}_{k'q'}=\frac{4\pi}{c}\frac{\mathbf{j}_{kq}^{ext}}{k^2+q^2}+\frac{\mathbf{g}_{kq}}{k^2+q^2}, \tag{5}$$

where $J_1(x)$ is the first order Bessel function. After summation over k

$$\mathbf{A}_q=\sum_k\mathbf{A}_{k,q}, \tag{6}$$

Eq. (5) transforms to

$$\mathbf{A}_q+\frac{2\pi R}{\Lambda}\sum\frac{J_1|\mathbf{q}-\mathbf{q}'|R}{|\mathbf{q}-\mathbf{q}'|}\mathbf{A}_{q'}=\frac{2\pi}{q^2}\mathbf{j}_q^{ext}+\frac{\mathbf{g}_q}{2q}. \tag{7}$$

The vectors $\mathbf{A}_q$, $\mathbf{j}_q$, and $\mathbf{g}_q$ can be expressed as

$$\mathbf{A}_q=i\frac{[\mathbf{q}\cdot\mathbf{z}_0]}{q}A_q,$$

$$\mathbf{j}_q^{ext}=i\frac{[\mathbf{q}\cdot\mathbf{z}_0]}{q}cH_{0\omega}R_0\frac{J_1(qR_2)}{2}, \tag{8}$$

$$\mathbf{g}_q=i\frac{[\mathbf{q}\cdot\mathbf{z}_0]}{q}2\pi\int_0^R rg(r)J_1(qr)dr.$$

Here $H_{0\omega}$ is the external field component at frequency ω in the cavity without the film and $\mathbf{z}_0$ is the unit vector aligned with the z-axis. Using the addition theorem for the Bessel functions,[25] we obtain

$$\frac{(J_1|\mathbf{q}-\mathbf{q}'|R)}{|\mathbf{q}-\mathbf{q}'|}=\frac{2}{R}\sum_{n=0,\ldots}^{\infty}(n+1)\times\frac{J_{n+1}(qR)}{q}\frac{J_{n+1}(q'R)}{q'}\frac{\sin[(n+1)\phi]}{\sin\phi},$$

where ϕ is the angle between q and q', and after integration with respect to ϕ we obtain

$$A_q+\frac{2\pi}{\Lambda}\sum_{n=2,4,\ldots}^{\infty}n\frac{J_n(qR)}{q^2}U_n=\frac{2\pi}{q^2}H_{0\omega}R_0J_1(qR_0)+\frac{g_q}{2q}, \tag{9}$$

where

$$U_n=\sqrt{n}\int_0^\infty J_n(qR)A_q dq. \tag{10}$$

Multiplication of Eq. (10) by $J_n(qr)$ and integration with respect to q yield

$$U_n+\frac{R}{\Lambda}\sum_{n'=2,4,\ldots}G_{nn'}U_{n'}=\frac{\pi H_{0\omega}R^2}{2\sqrt{2}}\delta_{2,n}+\sqrt{n}\int_0^\infty J_n(qR)g_q\frac{dq}{2q}, \tag{11}$$

where

$$G_{nn'}=\frac{1}{R}\int_0^\infty\frac{dq}{q^2}J_n(qR)J_{n'}(qR)=-\frac{4}{\pi}\frac{(-1)^{|n-n'|/2}}{((n+n')^2-1)((n-n')^2-1)}. \tag{12}$$

The vector potential component in the plane $z=0$,

$$A_\theta(r)=\int_0^\infty qJ_1(qr)A_q\frac{dq}{2\pi},$$

can be derived from Eq.(10):

$$A_\theta(r)=\frac{H_{0\omega}r}{2}-\frac{1}{\Lambda}\sum\sqrt{nU_n}Q_n+\frac{1}{2}\int_0^\infty dq\int_0^R dr'J_1(qr)J_1(qr')r'g_q(r'), \tag{13}$$

where

$$Q_n=\int_0^\infty\frac{dq}{2\pi q}J_1(qr)J_n(qR). \tag{14}$$

The system of equations (11) and (13) yields the vector potential $A_\theta(r)$ in the film expressed as a nonlinear function of the amplitude of the external field component $H_{0\omega}$:

$$A_\theta(r)=\Psi(r,H_{0\omega})H_{0\omega}. \tag{15}$$

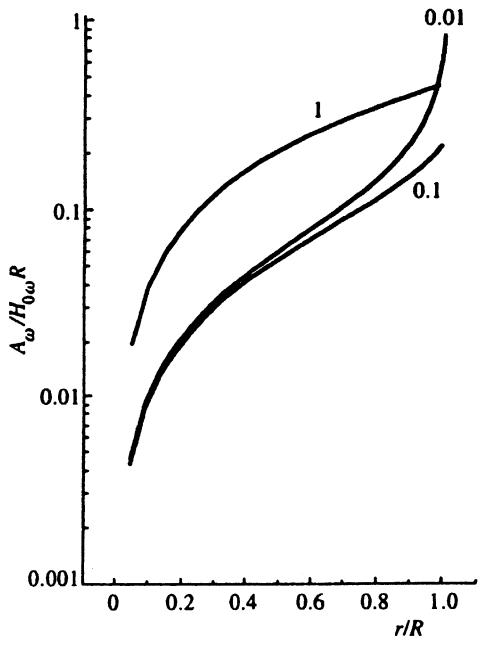

FIG. 6. Distribution of the vector potential over radius at several values of Λ/R (labeled curves).

Figure 6 shows calculations of the function $\Psi(r,H_{0\omega})$ in the low-field limit for several values of Λ/R.

4.2. Nonlinear response at low field amplitudes

Given the field distribution in the film in the linear approximation at an external field amplitude $H_{0\omega}$, we can calculate the intensity of the harmonic generated in the cavity by perturbation theory. Since the cavity is resonant in two modes, we only take their frequencies into account. In calculating the amplitude of the harmonic generated in the cavity, we describe the electromagnetic field in terms of electric E and magnetic H fields instead of vector potential. This approach is commonly applied to such problems.

We express the current as

$$j(\mathbf{r},t)=\sigma(\omega,\mathbf{r})E_\omega(\mathbf{r})\exp(-i\omega t)+\sigma(\omega_h,\mathbf{r})E_h(\mathbf{r}) \times\exp(-i\omega_h t)+\chi(\mathbf{r})E_\omega^3(\mathbf{r})\exp(-3\omega t)+\ldots, \quad (16)$$

where $E_h(\mathbf{r})$ and $\sigma(\omega_h,\mathbf{r})$ are the harmonic amplitude and conductivity at the harmonic frequency ω_h, respectively, and $\chi(\mathbf{r})$ is the nonlinearity parameter. The parameters σ and χ are, obviously, nonzero only in the film. If the effect of the normal current is negligible, then

$$\chi=\frac{ic^4}{2\pi\Lambda\omega^3}\frac{1}{(4\pi\Lambda^2 j_{GL})^2}. \quad (17)$$

The harmonic field satisfies the inhomogeneous linear Maxwell equations:

$$\text{curl}\,\mathbf{H}_h=\frac{i\omega_h}{c}\epsilon(\omega_h)\mathbf{E}_h+\mathbf{j}^{nl}, \quad (18)$$

$$\text{curl}\,\mathbf{E}_h=\frac{i\omega_h}{c}\mathbf{H}_h. \quad (19)$$

In these equations we use the notation $\epsilon(\omega_h)=1+4\pi i\sigma/\omega_n$ and $j^{nl}=\chi E_\omega^3$. We seek solutions of these equations in the form of expansions

$$\mathbf{E}_h=\sum a_s\mathbf{E}_s, \quad \mathbf{H}_h=\sum b_s\mathbf{H}_s \quad (20)$$

in terms of cavity eigenmodes $\mathbf{E}_s$ and $\mathbf{H}_s$, i.e., solutions of the homogeneous system

$$\text{curl}\,\mathbf{H}_s=-\frac{i\omega_s}{c}\epsilon(\omega_s)\mathbf{E}_s, \quad (21)$$

$$\text{curl}\,\mathbf{E}_s=\frac{i\omega_s}{c}\mathbf{H}_s. \quad (22)$$

After multiplying Eqs. (18) and (19) by $\mathbf{E}_s$ and $\mathbf{H}_s$, respectively, and performing simple transformations, including integration over the cavity, we obtain the expansion factors

$$a_s=\frac{\int\omega\mathbf{j}^{nl}\mathbf{E}_s dV}{(\omega_h^2-\omega_s^2)\int\epsilon E_s^2 dV}, \quad (23)$$

$$b_s=\frac{\int\omega_s\mathbf{j}^{nl}\mathbf{E}_s dV}{(\omega_h^2-\omega_s^2)\int\epsilon E_s^2 dV}. \quad (24)$$

Usually the experiment is conducted under resonant conditions, so that only one mode is excited at the harmonic frequency. By expressing the ratio of real and imaginary parts of the resonant frequency in terms of the Q-factor of the excited mode, $Q_s=\omega_s'/2\omega_s''$, we derive the following expression for the harmonic amplitude in this case:

$$a_s=-\frac{Q_s}{\omega_h}\int\mathbf{j}^{nl}\mathbf{E}_s dV. \quad (25)$$

For convenience we assume that resonant modes of the cavity are normalized by the condition

$$\int\epsilon E_s^2 dV=4\pi. \quad (26)$$

The field $E_s(\mathbf{r})$ of the resonant mode in the volume occupied by the film can be related to the field in the cavity without the film, $E_{0s}(\mathbf{r})$, through the function $\Psi(\mathbf{r},H_{0\omega})$ introduced by Eq. (15):

$$E_s(\mathbf{r})=\frac{H_s}{E_s}\frac{\omega}{c}\Psi(\mathbf{r},0)E_\omega(\mathbf{r}). \quad (27)$$

The harmonic amplitude is proportional to the cube of the incident-wave amplitude:

$$a_s\propto\chi dE_\omega^3\int\Psi^4(r,0)rdr. \quad (28)$$

Here integration is performed over the film volume. The parameter E_{0s} is assumed to be constant over the film. The Ginzburg–Landau equations yield a natural criterion of smallness of the incident-wave amplitude. The field intensity is low if the microwave current due to this field is small in comparison with the decoupling current j_{GL}. In the configuration used in the experiment, the highest current flows near

the film edge, and this is the area where the low-field criterion fails as the incident-wave amplitude increases.

4.3. Nonlinear response to a high-amplitude field

Perturbation theory does not apply in a strong field, and Eq. (28) is not valid. The main difference in the calculation of the harmonic intensity under a strong field is that it must take account of the incident-wave self-action, i.e., the function $\Psi(\mathbf{r},H_{0\omega})$ must be calculated at $H_{0\omega} \neq 0$. This means that one should calculate the vector potential in Eq. (13) with due account of nonlinear corrections as functions of the external uniform magnetic field. The harmonic intensity must be derived by solving the problem of a cavity driven by a given current that depends on the field amplitude at the fundamental frequency and contains all harmonics. Obviously, at low amplitude $H_{0\omega}$, the result will be the same as in the previous section, and at a higher amplitude the calculation will deviate from a cubic function.

One can try to find a relationship between the current and vector potential such that the experimental and theoretical curves coincide. Our data indicate that the fit is good when the field–current relation is described by curve *1* in the insert of Fig. 4. For comparison, the graph shows curve *2*, which demonstrates the relationship between the field and current derived from the Ginzburg–Landau phenomenological theory.

5. DISCUSSION

We now discuss experimental results. Our numerical calculations indicate that over a wide range of Λ/R from 5×10^{-4} to 5×10^{-2} the following approximation holds:

$$\int \Psi^4(r,0)rdr=0.46R^6(\lambda^2/Rd)^{2.85}. \qquad (29)$$

Given Eqs. (28) and (29), we can derive the temperature dependence of the penetration depth from the temperature dependence of the third harmonic amplitude plotted in Fig. 1. An important point is that the parameter χ in the Ginzburg–Landau theory is independent of temperature. The result of this procedure is shown in Fig. 7. The procedure, of course, only applies to the field intensity range where the third-harmonic amplitude is a cubic function of the incident-wave amplitude, i.e., at a low enough field intensity.

The reason for the maximum in the temperature curve in Fig. 1 is not entirely clear. Its position is too far from T_c, whereas in the simple model the signal should decrease over a temperature interval where λ is comparable to the normal skin depth, i.e., much closer to T_c. The maximum can scarcely be attributed to generation of vortices since the onset microwave field of this process should be a function of the film radius, whereas in our experiments the maximum positions for films of different sizes coincide.

The third-harmonic amplitude is a cubic function of the incident-wave intensity at low fields, and at higher amplitudes it deviates from the cubic function, the sign of this deviation depending on the temperature. Far from T_c the experimental curve is higher than the plot of the cubic function, and near T_c it is lower. Note that in our case the harmonic intensity has no threshold, unlike the similar effect detected in the radio-frequency[5,6] and kilohertz bands.[14,18]

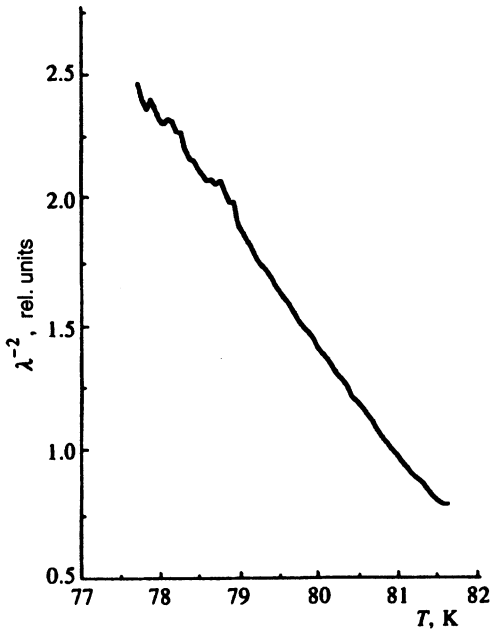

FIG. 7. Magnetic field penetration depth λ as a function of temperature.

At low incident-wave amplitudes, the most likely reason for harmonic generation is the nonlinearity in the Ginzburg–Landau equations, i.e., the drop in the order parameter due to the microwave field. Another possible reason for the nonlinearity is the existence of weak bonds. A dc magnetic field with an intensity of up to 200 Oe, however, did not result in a notable change in the signal. This leads us to conclude that the nonlinearity due to weak bonds between grains of the superconducting material is not important in this case, unlike the experiments reported in Refs. 26–29.

The deviation of experimental curves from cubic functions at high field intensities may be due to a number of effects, such as overheat, generation of vortices, and developed vortex-free nonlinearity. We now us discuss these effects in detail.

5.1. Overheat

The curves in Figs. 2–5 have been recorded at temperatures below the maximum in Fig. 1. In this temperature range, the sample overheat should lead to a harmonic intensity higher than that prescribed by the cubic curve. The experimental data indicate that it occurs in some cases, but in other cases the effect has the opposite sign, thus it cannot be comprehensively interpreted in terms of the overheat.

5.2. Generation of Abrikosov vortices

At high enough incident-field intensity, Abrikosov vortices can be generated in the film. The microwave frequency should be low enough so that the Meissner state can become unstable. The time needed to develop instability when the current at the film edge is higher than the decoupling current is of the same order of magnitude as the order parameter

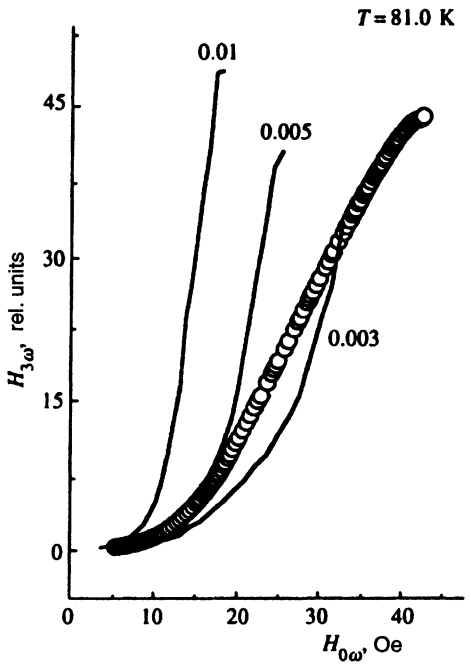

FIG. 8. Numerical calculations of the third-harmonic amplitude taking into account generation of vortices. The numbers labeling the curves are values of Λ/R.

relaxation time,[30] but the edge current should be comparable to the decoupling current. A simple estimate of their ratio, however, yields[24]

$$\frac{j(R)}{j_{GL}}=3^{3/2}\,\frac{H_{0\omega}R\xi(T)}{\Phi_0}(\lambda^2/Rd)^{0.54}\sim 0.1. \tag{30}$$

Here $H_{0\omega}$ is the microwave amplitude in the cavity at which the experimental curve deviates from the cubic function, and the estimates of the coherence length and penetration depth at $T=77$ K are taken from the review by Blatter *et al.*[31] The edge current in the range where the points deviate from the cubic curve is clearly much lower than the decoupling current, and there is no reason to invoke vortices in the homogeneous film model. The field amplitude at which vortices are generated in a film may be lower owing to inhomogeneities at the film edge.[23] Therefore we have calculated the third-harmonic intensity generated in the film using the previously developed numerical technique.[18] Calculations of the third-harmonic intensity at three different values of Λ/R taking into account generation of vortices are given in Fig. 8. The curves indicate that vortex nonlinearity should also lead to a higher harmonic intensity at all temperatures; therefore, like the overheat, this effect cannot account for the weaker than cubic behavior at temperatures below the maximum in Fig. 1.

5.3. Developed vortex-free nonlinearity

Equations (11) and (13) clearly indicate that the vector potential in the film is a nonlinear function of the external field amplitude, and this nonlinearity cannot be described by a simple cubic function in Eq. (6) throughout the range in question, even if $g(A)$ is a simple cubic function. This means that the third-harmonic amplitude versus field intensity should exceed the cubic curve. In order to obtain a deviation with the opposite sign, as observed in experiments, one has to modify the function $g(A)$. From this standpoint, experiments on generation of the third harmonic can be considered measurements of the current density as a function of the superfluid velocity at microwave frequencies. The function $j(A)$ fitted to the experimental data at a fixed temperature is plotted in Fig. 4. Certainly, the microscopic nature of this function remains unclear.

6. CONCLUSION

The third harmonic generated by a thin superconducting YBaCuO film in a microwave field normal to its surface has been experimentally investigated. Its intensity has been measured as a function of temperature and amplitude of the incident wave. We have demonstrated that, unlike the case of the low-frequency band, harmonic generation has no threshold, but harmonic intensity is a cubic function of the incident-field amplitude only at low microwave power.

We have developed a technique for calculating the harmonic intensity generated by a thin film in weak and strong microwave fields. At low amplitudes, the harmonic intensity versus temperature reflects the temperature dependence of the London penetration depth, thus providing a relatively simple method for studying magnetic field penetration.

The phenomenological relation between the current density and vector potential prescribed by the Ginzburg–Landau theory cannot account for the experimental curve of the third-harmonic intensity versus incident power at high microwave intensities.

The lack of a threshold in harmonic generation and the weak dependence on the dc magnetic field indicate that a vortex pattern either cannot be generated during the microwave field period or has no effect on the harmonic generation.

The authors are indebted to A. A. Varlamov, V. M. Vinokur, G. F. Zharkov, and A. E. Koshelev for helpful discussions, L. A. Mazo for supplying the samples, and M. G. Leviev for producing a user-friendly program for data collection.

The work was supported by the Council on High-T_c Superconductivity ("Nonlinearity") and International Science Foundation (Grant No. REH000).

[1] J. R. Delayen, C. L. Bohn, and C. T. Roche, J. Supercond. **3**, 243 (1990).
[2] P. P. Nguyen, D. E. Oates, G. Dresselhaus, and M. S. Dresselhaus, Phys. Rev. B **48**, 6400 (1993).
[3] G. C. Bailey and A. C. Ehrlich, Phys. Lett. A **92**, 457 (1982).
[4] I. I. Eru, V. A. Kashchei, and S. A. Peskovatskii, Zh. Éksp. Teor. Fiz. **58**, 778 (1970) [Sov. Phys. JETP **31**, 416 (1970)].
[5] S. A. Govorkov, S. K. Tolpygo, and V. A. Tulin, Zh. Éksp. Teor. Fiz. **89**, 1389 (1985), [Sov. Phys. JETP, **62**, 804 (1985)].
[6] V. A. Berezin, S. V. Govorkov, S. K. Tolpygo, and V. A. Tulin, Fiz. Tverd. Tela **17**, 246 (1985).
[7] A. H. Netercot and R. J. von Gutfeld, Phys. Rev. **131**, 576 (1963).
[8] K. Rose and M. D. Sherrill, Phys. Rev. **145**, 179 (1963).
[9] L. P. Gor'kov and G. M. Éliashberg, Zh. Éksp. Teor. Fiz. **56**, 1297 (1969) [Sov. Phys. JETP **29**, 698 (1969)].
[10] I. O. Kulik, Zh. Éksp. Teor. Fiz. **57**, 600 (1969) [Sov. Phys. JETP **30**, 329 (1969)].
[11] G. I. Leviev, A. V. Rylyakov, and M. R. Trunin, JETP Lett. **50**, 88 (1989).

[12]I. Ciccarello, C. Fazio, M. Guccione, and M. Li Vigni, Physica C **159**, 769 (1989).
[13]M. W. Coffey and J. R. Clem, Phys. Rev. B **48**, 342 (1993).
[14]L. Ji, R. H. Sohn, G. C. Spalding *et al.*, Phys. Rev. B **40**, 10936 (1989).
[15]I. Ciccarello, C. Fazio, M. Guccione *et al.*, Phys. Rev B **49**, 6280 (1994).
[16]L. A. Vainshtein, *Electromagnetic Waves* [in Russian], Nauka, Moscow (1988).
[17]P. N. Mikheenko and Yu. E. Kuzovlev, Physica C **204**, 229 (1993).
[18]E. S. Bakhanova, V. M. Genkin, S. N. Konkin, and S. A. Churin, Zh. Éksp. Teor. Fiz. **100**, 1919 (1991) [JETP **73**, 1061 (1991)].
[19]P. de Gennes, *Superconductivity of Metals and Alloys*, W. A. Benjamin, Inc., New York–Amsterdam (1966).
[20]J. Pearl, Appl. Phys. Lett. **5**, 65 (1964).
[21]E. Zeldov, A. I. Larkin, V. B. Geshkenbein *et al.*, Phys. Rev. Lett. **73**, 1428 (1994).
[22]M. V. Indenbom and E. H. Brandt, Phys. Rev. Lett. **73**, 1731 (1994).
[23]K. K. Likharev, Izv. Vyssh. Uchebn. Zaved., Radiofizika **14**, 909, 919 (1971).
[24]E. S. Borovitskaya and V. M. Genkin, Physica C (1996).
[25]E. Janke, F. Emde, and F. Lösch, *Special Functions* [Russian translation], Nauka, Moscow (1977).
[26]A. M. Portis, D. W. Cooke, E. R. Gray *et al.*, Appl. Phys. Lett. **58**, 307 (1991).
[27]D. W. Cooke, P. N. Arendt, E. R. Gray *et al.*, Appl. Phys. Lett. **58**, 1329 (1991).
[28]B. Bonin and H. Safa, Supercond. Sci. Technol. **4**, 257 (1991).
[29]Yu. M. Ivanchenko, A. A. Lisyanskii, and M. I. Tsindlekht, Zh. Éksp. Teor. Fiz. **97**, 329 (1990). [Sov. Phys. JETP **70**, 187 (1990)].
[30]L. G. Aslamazov and S. V. Lempitskii, Zh. Éksp. Teor. Fiz. **84**, 2216 (1983) [Sov. Phys. JETP **57**, 1291 (1983)].
[31]G. Blatter, M. V. Feigel'man, V. B. Geshkenbein *et al.*, Rev. Mod. Phys. **66**, 1125 (1994).

Translation was provided by the Russian Editorial office.